VBench: Comprehensive Benchmark Suite for Video Generative Models

Supplementary Material

In this ***supplementary file***, we provide more details on *Evaluation Dimension Suite* and *Evaluation Method Suite* in Section A, and elaborate on *Prompt Suite* details in Section B. We then provide further explanations on *Human Preference Annotations* in Section C, and more implementation details on our experiments and visualizations in Section D. The potential societal impacts of our work are discussed in Section E. We also discuss our limitations in Section F. Finally, in Section G, we provide additional experimental results used to support the visualizations and insights in the main paper.

A ***demo video*** is also provided along with this supplementary file to illustrate VBench and show video examples of each dimension.

A. More Details on Evaluation Dimension and Method Suite

A.1. Video Quality

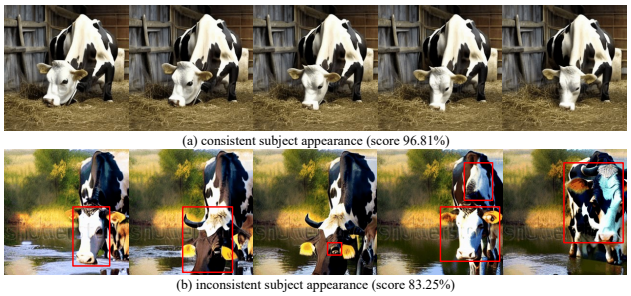

Figure A1. **Visualization of *Subject Consistency***. We demonstrate different degrees of subject consistency, as indicated by our *Subject Consistency* score (the larger the better) **(a)** The cow has a relatively consistent look throughout across different frames. **(b)** The cow shows inconsistency in its appearance over time. The red boxes indicate areas of subject inconsistency.

Subject Consistency. When there is a subject (*e.g.*, a cow, a person, a car, or a cat) in the video, it is important that the subject looks consistent throughout the video (*i.e.*, whether it is still the same thing or the same person). For example, in Figure A1, the cow in the top row remains consistent across different frames, while the cow in the bottom row shows changes in appearance between frames. To evaluate subject consistency, we employ DINO [7] to extract features from each frame to represent the subject. Since DINO is not trained to disregard the differences within subjects of the same class [52], its feature extraction is particularly sensitive to the identity variations of the subject within the video, thereby making it a suitable tool for evaluating subject consistency. Specifically, for each video, the subject consistency score is calculated as:

$$S_{subject} = \frac{1}{T-1}\sum_{t=2}^{T}\frac{1}{2}(\langle d_1 \cdot d_t\rangle + \langle d_{t-1} \cdot d_t\rangle), \quad (1)$$

where d_i is the DINO image feature of the i^{th} frame, normalized to unit length, and $\langle\cdot\rangle$ is the dot product operation for calculating cosine similarity. For each frame, we calculate the cosine similarity with the first frame and its preceding frame, take the average, and then compute the mean over all the non-starting video frames. We average the score $S_{subject}$ for all the videos generated by one model as the final score of the model.

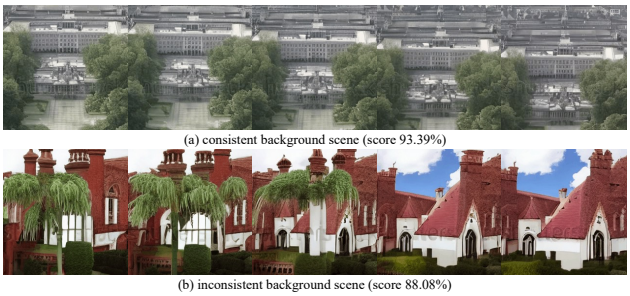

Figure A2. **Visualization of *Background Consistency***. We showcase varying levels of background consistency, as indicated by our *Background Consistency* metrics (larger values denote better consistency) **(a)** The background scene maintains a high degree of consistency (*i.e.*, still the same scene) across different frames. **(b)** The background exhibits noticeable distortion and abrupt changes over time.

Background Consistency. Beyond the focus on the foreground subject, maintaining a consistent background scene across different frames is equally important. For example, in Figure A2, in the top row, the scene maintains a consistent appearance as the camera moves, while in the bottom row, the entire scene undergoes significant changes within a few frames. For each video frame, we employ the CLIP [50] image encoder to extract its feature vector. We then compute the background consistency metric, which is similar to the method used for *Subject Consistency*:

$$S_{background} = \frac{1}{T-1}\sum_{t=2}^{T}\frac{1}{2}(\langle c_1 \cdot c_t\rangle + \langle c_{t-1} \cdot c_t\rangle), \quad (2)$$

where c_i represents the CLIP image feature of the i^{th} frame, normalized to unit length.

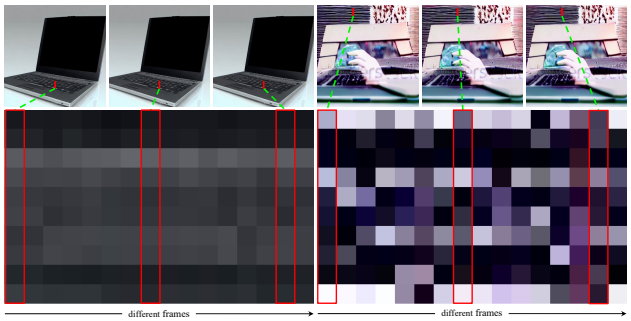

(a) mild flickering (score 99.68%) (b) serious flickering (score 96.01%)

Figure A3. **Visualization of *Temporal Flickering*.** We demonstrate different degrees of temporal flickering, with a mild occurrence in (a), and a severe occurrence in (b), both reflected by our flicker score metrics (the larger the better). To visualize temporal flickering, given a generated video (***top row***), we extract a small segment of pixels (marked as the red segment) from each frame at the same location and stack them in frame order (***bottom row***). **(a)** Pixel values do not vary abruptly, and the video suffers less from flickering. **(b)** Pixel values vary abruptly and frequently across different frames, showing strong temporal flickering. Our evaluation metrics also give a lower score.

Table A1. ***Dynamic Degree* on Three Benchmarks.** We report the *Dynamic Degree* metrics on three *Temporal Flickering* benchmarks. We use videos from the Subject Consistency dimension as the "Dynamic Benchmark", videos from the Background Consistency dimension as the "Semi-Dynamic Benchmark", and videos from the temporal flickering dimension as the "Static Benchmark".

Models	Static Benchmark	Semi-Dynamic Benchmark	Dynamic Benchmark
LaVie [61]	0.00%	6.51%	49.72%
ModelScope [42, 56]	0.00%	33.72%	66.39%
VideoCrafter [23]	0.00%	51.63%	89.72%
CogVideo [25]	0.00%	14.19%	42.22%

Temporal Flickering. For real videos, temporal flickering is usually a result of frequent lighting variation, or shaky camera motions during the video capture process. However, for generated videos, temporal flickering is an intrinsic property of the video generation model, usually caused by imperfect temporal consistency at local and high-frequency details. In generated videos, temporal inconsistency can be attributed to various types of issues, including temporal flickering, unnatural motions, subject inconsistency *etc*. To disentangle the evaluation of temporal flickering from other aspects, we use static video scenes (*i.e*., no apparent motions) as the test cases (We use carefully designed prompts to generate static scenes for video sampling. To further ensure that the evaluation is conducted on static videos without apparent motions, we employ an optical flow estimator [55] to filter out videos and only keep the static videos). We calculate the frame-by-frame temporal flickering degree

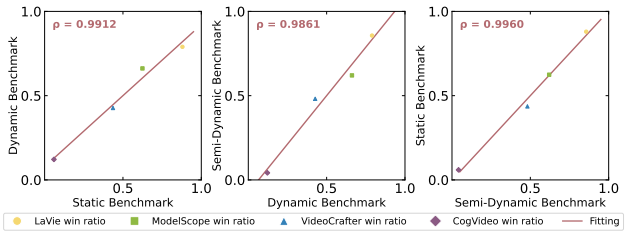

Figure A4. **Temporal Flickering Human Preference across Different Dynamic Degrees.** In each plot, a dot represents the human preference win ratio, where the horizontal and vertical axes correspond to two different benchmarks with different dynamic degrees. We linearly fit a straight line to visualize the correlation and calculate the correlation (ρ) for each dimension. We observe that the human preferences in terms of temporal flickering on these three benchmarks have high mutual correlations of around 99%.

with the following formula:

$$S_{flicker} = \frac{1}{N}\sum_{i=1}^{N}\left(\frac{1}{T-1}\sum_{t=1}^{T-1} MAE(f_i^t, f_i^{t+1})\right), \quad (3)$$

where N is the number of videos generated by a model, T is the number of frames per video, f_i^t is the frame t in video i, and MAE is the Mean Absolute Error between two consecutive frames over all pixel locations. We then normalize the temporal flickering degree to $[0, 1]$ as follows:

$$S_{flicker-norm} = \frac{255 - S_{flicker}}{255}, \quad (4)$$

where a higher score implies less flickering, and thus better video perceptual quality in terms of temporal flickering.

To verify that the strength of motions (*i.e*., large motion or small motion) in videos does not significantly impact the model's ranking in terms of temporal flickering, we conduct separate human evaluations for the level of temporal flickering on videos with different dynamic degrees, and show in Figure A4 that model ranking in terms of temporal flickering does not vary based on the dynamic degree of test videos. For videos of high dynamic degrees, we use videos from the *Subject Consistency* dimension's prompt suite, and term as the "Dynamic Benchmark". For videos that exhibit lower dynamic degrees but remain non-static, we use videos sampled from the *Background Consistency* dimension's prompt suite, and label them as the "Semi-Dynamic Benchmark". Additionally, the "Static Benchmark" refers to the videos sampled from the prompt suite for the *Temporal Flickering* dimension. We show the dynamic degree of videos in these three benchmarks in Table A1. In Figure A4, we show that the human win ratio in terms of temporal flickering on three benchmarks is almost perfectly correlated with each other, with a correlation of around 99% between any two benchmarks. Therefore, we believe the

degree of motion is disentangled with the temporal flickering ranking in video generative models, and we use the "Static Benchmark" for easier and more focused evaluation on *Temporal Flickering*.

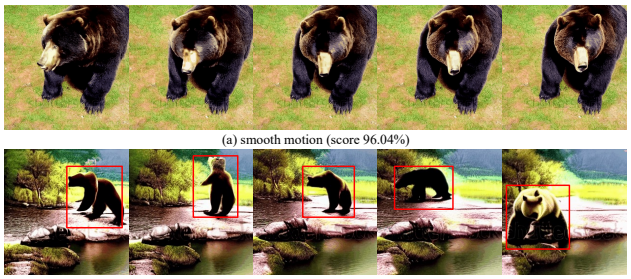

(a) smooth motion (score 96.04%)

(b) unnatural motion (score 88.47%)

Figure A5. **Visualization of *Motion Smoothness***. We investigate various levels of motion smoothness, ranging from being smooth as depicted in (a) to highly erratic as depicted in (b), as indicated by our motion score metrics (larger values denote better smoothness). The red boxes indicate areas of discontinuous motion.

Motion Smoothness. To evaluate whether the motion in the generated video is smooth and follows the physical law of the real world, we make use of the frame-by-frame motion prior to video frame interpolation models. Specifically, video frame interpolation models usually assume real-world motions within a very short time period (*i.e.*, a few consecutive frames) to be linear or quadratic and synthesize the non-existing intermediate frames based on this assumption. Given a generated video consisting of frames $[f_0, f_1, f_2, f_3, f_4 ..., f_{2n-2}, f_{2n-1}, f_{2n}]$, we manually drop the odd-number frames to obtain a lower-frame-rate video $[f_0, f_2, f_4 ..., f_{2n-2}, f_{2n}]$, and use video frame interpolation [38] to infer the dropped frames $[\hat{f}_1, \hat{f}_3, ..., \hat{f}_{2n-1}]$. We then compute the Mean Absolute Error (MAE) between the reconstructed frames and the original dropped frames. The calculated MAE is normalized in the same way as Equation 4, so that the final score falls into $[0, 1]$, with a larger number implying smoother motion.

Dynamic Degree. Based on our observations, some models tend to generate static videos even when the prompt includes descriptions of movement. This results in a noticeable advantage for these models in evaluations of other temporal consistency dimensions, leading to unfair comparisons. This dimension is designed to assess the extent to which models tend to generate non-static videos. We use RAFT [55] to estimate optical flow strengths between consecutive frames of a generated video. We then take the average of the largest 5% optical flows (considering the movement of small objects in the video) as the basis to determine whether the video is static. The final dynamic degree score is calculated by measuring the proportion of non-static videos generated by the model.

Aesthetic Quality. Aesthetic Quality takes photographic layout rules, the richness and harmonies of colors, the artistic quality of the subjects, etc into account. We adopt an image aesthetic quality predictor to evaluate the generated videos frame by frame. We use the LAION aesthetic predictor [34] to give a 0-10 rating for each frame, linearly normalize the score to 0-1, and calculate the average score of all synthetic frames as the final video aesthetic score.

Imaging Quality. Imaging quality mainly considers the low-level distortions presented in the generated video frames *(e.g., over-exposure, noise, blur)*. We use the MUSIQ [32] image quality predictor trained on the

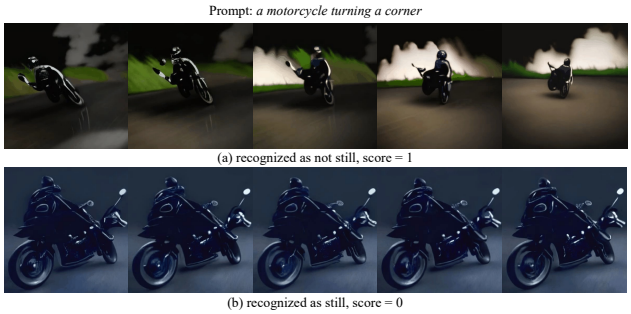

(a) recognized as not still, score = 1

(b) recognized as still, score = 0

Figure A6. **Visualization of *Dynamic Degree***. We present generated examples of different degrees of motion. **(a)** In the video, there is obvious motion of the camera and the object, which is identified as dynamic. **(b)** The video remains almost unchanged from the start to the end and is identified as static.

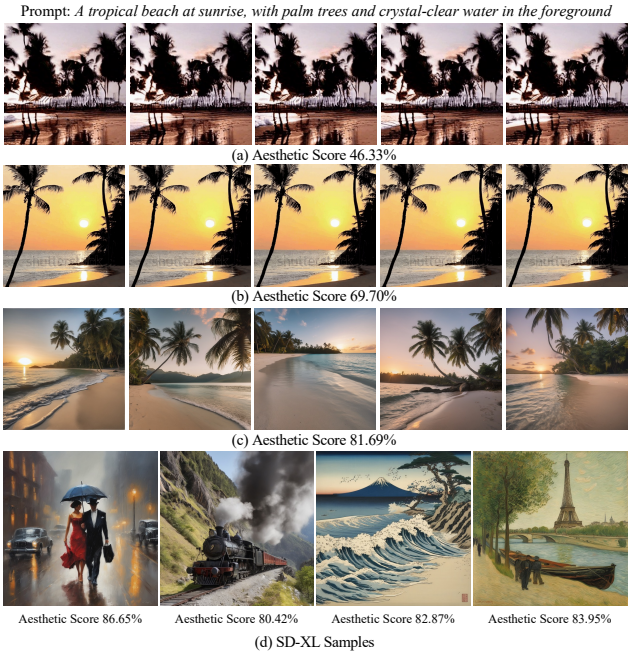

(a) Aesthetic Score 46.33%

(b) Aesthetic Score 69.70%

(c) Aesthetic Score 81.69%

(d) SD-XL Samples

Figure A7. **Visualization of *Aesthetic Quality***. We demonstrate video frames with varying degrees of aesthetic quality in (a), (b), and (c), which are effectively reflected by our aesthetic score metrics (higher indicating better). In (d), we showcase images with high aesthetic scores sampled from SDXL [48].

SPAQ [18] dataset, which is capable of handling variable-sized aspect ratios and resolutions. The frame-wise score is linearly normalized to $[0, 1]$ by dividing 100, and the final score is then calculated by averaging the frame-wise scores across the entire video sequence.

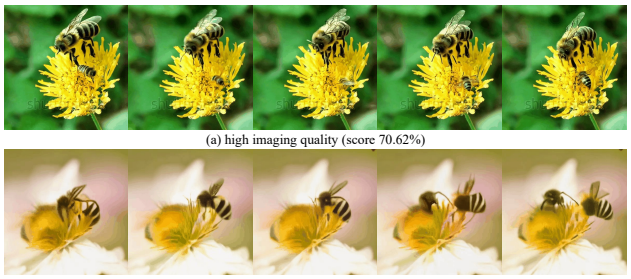

(a) high imaging quality (score 70.62%)

(b) low imaging quality (score 31.27%)

Figure A8. **Visualization of *Imaging Quality***. We present examples of generated videos with high imaging quality scores in (a), and low imaging quality scores (where the video is blurry and over-exposed) in (b).

A.2. Video-Condition Consistency

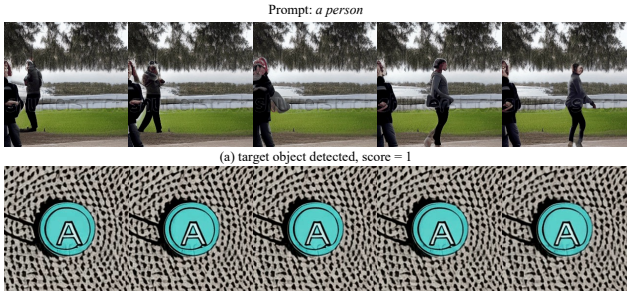

(a) target object detected, score = 1

(b) target object not detected, score = 0

Figure A9. **Visualization of *Object Class***. We demonstrate generation examples for the target object at varying degrees, as reflected by the object score metrics (where 1 represents success, and 0 represents failure). **(a)** The target object "person" is successfully generated in the video. **(b)** The synthesized video does not contain the target object.

Object Class. When a user specifies a certain type of object in the text prompt, we aim to evaluate whether the model can generate an object of the specified type. To this end, we use GRiT [65] to detect objects in each frame of the generated video and check whether the specified object class is successfully detected in these frames. Subsequently, we report the proportion of frames in which the corresponding object class has been successfully detected. We employ GRiT for this dimension, as well as several other semantics dimensions such as *Multiple Objects*, *Color*, and *Spatial Relationship* for two reasons: *1)* GRiT is a versatile framework that can handle both detection and captioning tasks, predicting diverse object attributes, so that the VBench can use the same framework across different dimensions and save users from installing multiple frameworks or downloading multiple pre-trained models. *2)* GRiT demonstrates reliable performance in evaluating our designated dimensions, with comparable performance with the state-of-the-art object detectors [65], and good alignment with human perception in terms of "correct detection" as validated by the human preference results in main paper Figure 5.

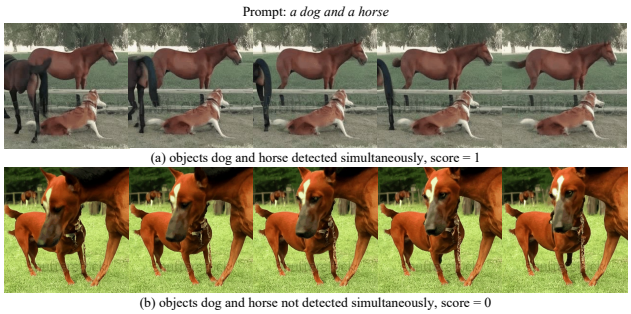

(a) objects dog and horse detected simultaneously, score = 1

(b) objects dog and horse not detected simultaneously, score = 0

Figure A10. **Visualization of *Multiple Objects***. We showcase instances of generating multiple objects within a video simultaneously at different levels, as indicated by our multiple objects score metrics (where 1 signifies success, and 0 denotes failure). **(a)** The video effectively generates multiple required objects (*i.e.*, dog and horse). **(b)** The video fails to produce the dog and horse at the same time.

Multiple Objects. Other than generating a single object, compositionality is also an essential aspect of video generation. Suppose the user requires generating multiple objects, we use GRiT for frame-wise object detection. For each frame, we check whether all the user-requested objects simultaneously appear in each frame. We then report the proportion of frames in which all the required objects have been successfully detected.

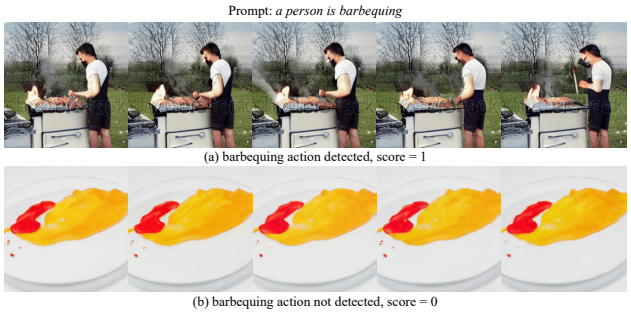

(a) barbequing action detected, score = 1

(b) barbequing action not detected, score = 0

Figure A11. **Visualization of *Human Action***. We showcase examples of generating the target action at different levels, as indicated by our action score metrics (where 1 denotes success, and 0 denotes failure). **(a)** The video successfully generates the barbequing action. **(b)** The video does not generate the target action.

Human Action. In the process of video synthesis from textual prompts, both the mentioned subjects in the prompt and the corresponding actions they engage in are important.

Given the remarkable emergence of high-quality human-centric generated videos, we believe it is necessary to ensure that human subjects depicted in videos accurately execute the specific actions described by the textual prompts. To this end, we use the Kinetics-400 dataset [31] as a reference due to its comprehensive characterization of diverse human actions. To evaluate the accuracy of the generated videos, we uniformly sample 16 frames from each video and apply UMT [37], which achieves the state-of-the-art classification performance on the Kinetics-400 dataset among open-sourced models to classify the action. The top 5 results with logits bigger than 0.85 are preserved as ground-truth candidates, and we check whether the actions mentioned in the text prompt appear in the ground-truth candidates. The average percentage of all classification results is reported to assess whether the generated videos have human actions aligned with the text prompts.

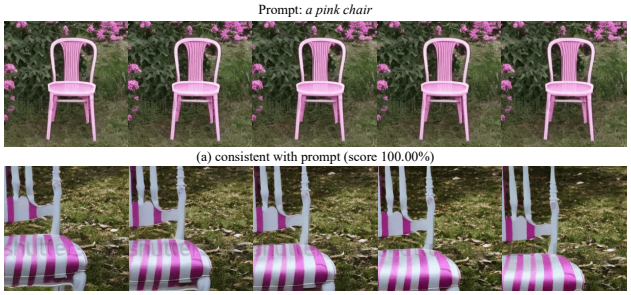

Figure A12. **Visualization of *Color***. We present examples of generating the target color within videos, depicting various levels of success through our color score metrics (larger denotes better). **(a)** The video accurately generates the target color. **(b)** The video only generated the target color in certain parts.

Color. To evaluate whether the color of an object is consistent with the specified condition, we use GRiT's captioning ability to describe colors, with slight modification to the GRiT pipeline. To remove the influence of the *Object Class* dimension's ability, we only consider videos where the object has been successfully generated. Specifically, GRiT identifies the bounding boxes of objects, which are then fed to two text decoders: one for predicting categories and the other for generating dense captions on the synthesized video frame. We then verify if the corresponding object's color is successfully captioned in all frames. Among the frames where the corresponding object is generated and the caption contains color information, we compute the percentage of frames where the color required by the text prompt is successfully captioned.

Spatial Relationship. We focus on *left-right* and *top-bottom* relationships and evaluate whether the video content adheres to the spatial relationship specified by the text prompts. Inspired by the T2I-CompBench [28] evaluation, we compute the spatial relationship accuracy based on the

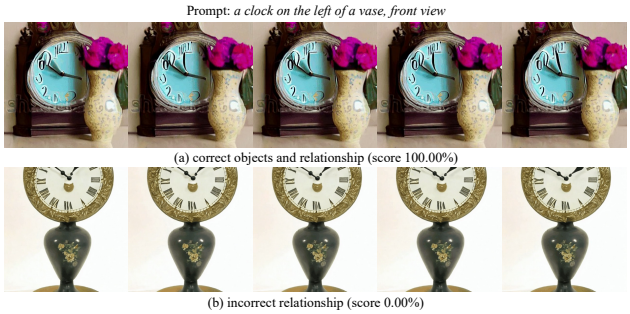

Figure A13. **Visualization of *Spatial Relationship***. We show examples of generating the spatial relationships mentioned in the prompt within videos. **(a)** The video successfully captures the spatial relationship and objects described in the prompt. **(b)** The generated video does not contain the intended relationship.

horizontal and vertical positioning of object pairs. During evaluation, distances on the designated axis (e.g., left-right) are expected to be greater than those on the other orientation (e.g., top-bottom). Under this condition, we observe the intersection over the union metric (IoU) of two objects to obtain the final score, where IoU values that fall below a specified threshold result in a score of 100%, and the values exceeding the threshold are multiplied by a coefficient based on the IoU to determine the final score. We use GRiT to detect the objects and their locations within the generated video frames, and we also calculate the Intersection over Union (IoU) of the two objects' bounding boxes as the final spatial relationship score coefficient.

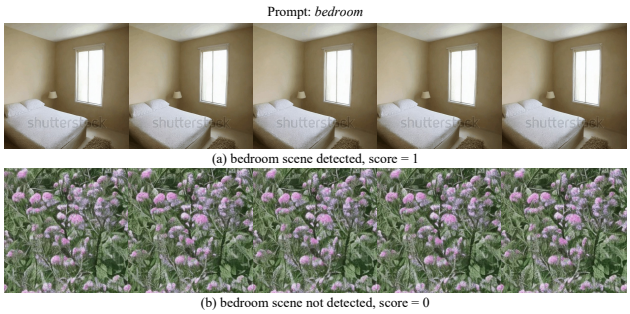

Figure A14. **Visualization of *Scene***. We present examples of generating the required scene (where 1 represents success, and 0 indicates failure). **(a)** The required scene is generated successfully. **(b)** The video does not show the scene as required.

Scene. For a scenario described by the text prompt, we need to evaluate whether the synthesized video is consistent with the intended scene. For example, when prompted to "ocean", the generated video should be "ocean" instead of "river". We use Tag2Text [29] to caption the generated scenes, and then check the correspondence with scene descriptions in the text prompt. Specifically, each word related to the scene in the text prompt needs to appear in the predicted caption, but the word order can be different. We then

report the proportion of frames in which the corresponding scene has been successfully generated.

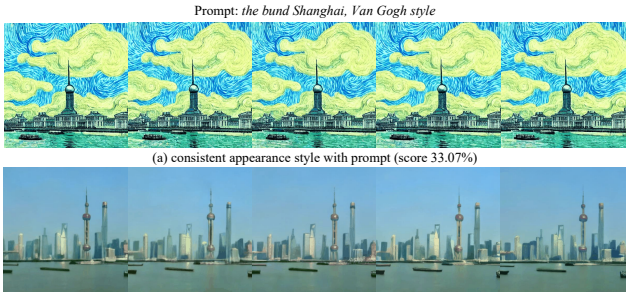

(a) consistent appearance style with prompt (score 33.07%)

(b) inconsistent appearance style with prompt (score 20.93%)

Figure A15. **Visualization of *Appearance Style***. We demonstrate examples of generating the required appearance style within videos, showcasing different levels of success as assessed by our appearance style score metrics. **(a)** The generated video follows the requested Van Gogh style. **(b)** The video does not show the desired appearance style.

Appearance Style. For stylized video generation, we first extract the style description in the text prompt, then evaluate the video-text feature similarity to assess appearance style consistency. Specifically, We use CLIP [50] to extract features from each frame and the text, and then compute the mean cosine similarity of the normalized features. CLIP demonstrates robust zero-shot performance in perceiving textual descriptions of styles, aiding our evaluation of style consistency.

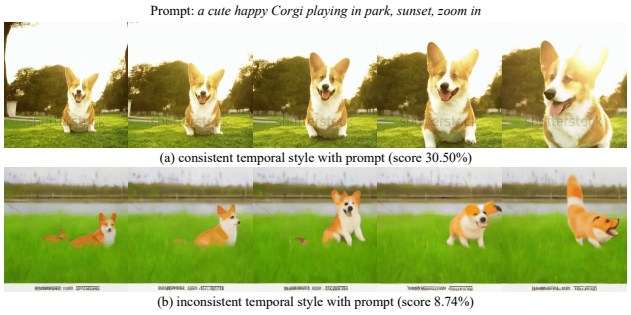

(a) consistent temporal style with prompt (score 30.50%)

(b) inconsistent temporal style with prompt (score 8.74%)

Figure A16. **Visualization of *Temporal Style***. We demonstrate two different generated videos to show the consistency of their temporal style with the prompt at various degrees, measured by our temporal style score. **(a)** The generated video follows the "zoom in" temporal style. **(b)** The video's temporal style does not align with the prompt.

Temporal Style. In videos, style is not only spatially narrated in individual frames, but also temporally revealed in different types of object motions and camera motions. For example, we are interested in whether the text prompt specifies "zoom in" or "zoom out", "pan left" or "pan right", and whether the generated video can show such kind of camera motion. Additionally, there are different types of other temporal styles like "super slow motion", "camera shaking", and "racking focus". In terms of temporal awareness, ViCLIP [62] is pre-trained on a diverse 10M video-text dataset, which shows strong zero-shot learning capabilities in video-text retrieval tasks. When a video is generated based on a specified temporal style, we use ViCLIP to calculate the video-text feature similarity to reflect temporal style consistency.

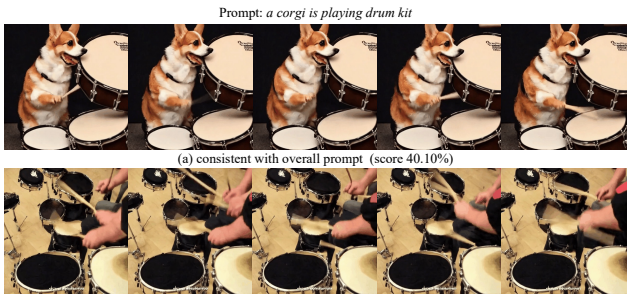

(a) consistent with overall prompt (score 40.10%)

(b) inconsistent with overall prompt (score 28.87%)

Figure A17. **Visualization of *Overall Consistency***. We demonstrate different examples that illustrate the extent to which they align with the prompt, as measured by our overall score metrics (larger values denote better consistency). **(a)** The video aligns closely with the prompt. **(b)** The video lacks alignment with the target concept.

Overall Consistency. We also use overall video-text consistency computed by ViCLIP as an aiding metric to reflect both semantics and style consistency, where the text prompts contain different semantics and styles.

B. More Details on Prompt Suite

B.1. Prompt Suite per Evaluation Dimension

For each VBench dimension, we carefully designed around 100 prompts as the test cases. *For semantics-related prompt suites, we provide clear semantics labels to each prompt in the prompt suites to facilitate efficient and accurate evaluation.* For example, we provide the object class labels for prompt suites of *Object Class*, *Multiple Objects*, and *Spatial Relationship*. We also provide color labels for *Color* prompts, relationship tags for *Spatial Relationship* prompts, and style labels for *Appearance Style*. We detail the prompt suite for each dimension as follows.

Subject Consistency. We choose 19 representative living or movable object categories from the COCO [40] dataset's 80 object categories. These categories encompass animals and transportation-related items. Each object category is associated with a set of carefully crafted actions or movements, ensuring logical coherence between the actions and their respective objects. A list of distinct prompts used for evaluating subject consistency is therefore created.

Background Consistency. We carefully select a list of distinct and representative scenes from the Places365 [79] dataset, aiming to include a diverse set of scenes within a

limited number of prompts. The selected scenes contain indoor, modern, rural, and various other settings, thereby ensuring the representation of a wide range of environmental contexts. This prompt suite is applied to both the *Background Consistency* dimension and the *Scene* dimension.

Temporal Flickering. To more effectively evaluate temporal flickering, it is essential to eliminate interference from other temporal dimensions. According to observations in Section A, whether the scene is static does not affect the temporal flickering ranking among models. Ultimately, we selected a set of prompts, covering various topics, scenarios, and prompt lengths. Each prompt is accompanied by a prefix instructing the model to generate a static scene.

Motion Smoothness. Since *Subject Consistency*'s prompt suite involves movements performed by different subjects, they serve as a good benchmark for *Motion Smoothness* as well. To minimize the number of videos needed to be sampled for each model in evaluation, we share the same prompt suite for both dimensions.

Dynamic Degree. Considering the issue of the model tending to generate static videos even when prompted with descriptions of motion, we use the same prompt suite as *Subject Consistency*'s, which includes a variety of motion descriptions.

Object Class. We use the COCO dataset [40] and drop the object `mouse`, due to the potential confusion as it can be interpreted as both device and animal. We then append articles to the rest of the 79 objects and create a list of prompts related to different object classes.

Multiple Objects. We categorize COCO objects into various groups so that it will be reasonable for them to appear together. These categories include animals, indoor items, dining objects, bathroom items, and outdoor items. We then generate a list of prompts by composing objects within each category.

Human Action. From the Kinetics-400 dataset [31], we carefully extract a subset of 100 actions by considering both diversity and minimal overlaps in their meanings. Our approach involves selecting only the actions that are unique. For instance, within the category of actions related to playing musical instruments, we only keep those actions that are considered dissimilar in terms of human posture and actions. The resulting selection contains a wide spectrum of actions. Subsequently, we integrate each action in the form of "a person is doing something", and craft a list of human-centric action prompts.

Color. We select representative classes from COCO objects and establish the color scope of our prompt suite. On the selection of objects, we select objects that are unique in shape and similar objects. For example, "skateboard" and "surfboard" are excluded due to their similar shapes and potential wrong detection results by detection models. A similar criterion is applied to the color selection, we aim to select colors to include a broad spectrum while avoiding closely related colors. For example, "gold" and "yellow" are considered similar, therefore we only include "yellow" in our color scope. Our prompts are generated by combining each object with a few of their typical colors, and we only keep objects with more than three typical colors.

Spatial Relationship. We organize COCO objects into different groups so that it is natural for them to be composed in the same scene with each other. Some examples of the categories include personal items, animals, and sports-related items. Additionally, we define relationship categories to be "left and right" and "top and bottom". We then select relationships that are reasonable for the objects within each category, resulting in a list of prompts designed to describe spatial relationships between objects.

Scene. We use the same prompt suite as *Background Consistency*, as both requires prompts describing different general scenes.

Appearance Style. We select a list of sentences covering a wide range of scenarios and themes and also define our list of appearance styles. The styles are carefully crafted to ensure diversity. For example, we include the representative "Van Gogh style" and traditional "Ukiyo style" for the clear contrast in their color schemes, brushwork techniques, and overall aesthetic expressions. Each scenario description is then composed with a list of appearance styles to form the prompts.

Temporal Style. We carefully curate a diverse list of representative temporal styles to represent a broad spectrum of camera movement and temporal effects commonly employed in video production. Our selected temporal styles include variations in motion speed, camera perspective, and dynamic effects, aiming to present a comprehensive range of cinematic techniques. Each sentence for a scenario is then composed with a list of temporal styles.

Overall Consistency. We create a range of prompts, covering different content categories and scenarios such as "natural scenery", "fantasy and sci-fi", "character and fictional beings" *etc*., these prompts are of varied length, and we include both general and specific descriptions in our prompts.

B.2. Prompt Suite per Category

In Section 3.2 of the main paper on *Prompt Suite Per Category*, we employ LLM [78] as the first step to categorize the collection of human-curated prompts into eight content categories. The input template for the language model is shown in Table A2. The accuracy of classification is around 95%, and we manually go through each classified prompt to filter out 100 prompts for each content category.

Animal. These prompts focus on various animals and their behaviors in different environments, such as "a frog eating an ant", "a harbour seal swimming near the shore", and "a squirrel eating nuts". This prompt suite captures diverse

The assistant gives helpful, detailed, and polite answers to the user's questions. Please act as a language expert, able to choose one or more suitable categories from [`Animal, Architecture, Food, Human, Lifestyle, Plant, Scenery, Vehicles`] for the given text. Given the input text, you should return the answer without explanation. For example, if the input is [`A man eats hamburgers.`], the output tag format should be [`Food, Human`].
The given text is `Input text`.

Table A2. **Category Classification.** We employ LLM to determine the content categories of collected text descriptions.

species from domestic pets to wild animals in various activities, such as feeding, playing, or simply existing in their natural or adapted environments.

Architecture. We keep prompts that include various types of architecture, including the different types of buildings and structures, such as "the view of the Sydney opera house from the other side of the harbor", "illuminated tower in Berlin", and "a tree house in the woods".

Food. These prompts are diverse and all revolve around food and beverages. They range from specific dishes and preparation methods to more conceptual food art and eating scenarios. Examples include "Freshly baked finger-licking cookies", "A person slicing a vegetable", and "Close-up video of Japanese food".

Human. These prompts describe a wide range of human activities, interactions, and scenes, each focusing on specific individuals or groups engaged in various actions. Here are some examples: "A family wearing paper bag masks", "Boy sitting on grass petting a dog", "Group of people protesting", and "Father and son holding hands". Each of these prompts paints a vivid picture of human life, capturing diverse moments from daily activities to special events, professional settings to personal interactions.

Lifestyle. These prompts describe various indoor scenes and activities, covering a wide range of settings and situations. For instance, "Interior design of the bar section" and "Dog on floor in room" are simple everyday indoor scenes. Each prompt captures a specific aspect of indoor life, ranging from personal moments and family interactions to professional and leisure activities, reflecting the diversity of experiences within indoor lifestyles.

Plant. These prompts mainly focus on plants and trees. Here are some examples: "Video of an indoor green plant", "A coconut tree by the house", and "Variety of trees and plants in a botanical garden".

Scenery. These prompts describe various natural and urban landscapes, each capturing a distinct aspect of the environment. Here are some examples: "View of the sea from an abandoned building", "Aerial footage of a city at night", and "Scenery of desert landscape". Each prompt can be of natural settings like beaches and mountains, the structured scenery of agricultural lands, or urban environments.

Vehicles. These prompts depict various forms of transportation and related scenes, including various vehicles like trains, cars, buses, motorcycles, and boats in diverse settings ranging from urban streets to natural landscapes. Here are some examples: "A modern railway station in Malaysia used for public transportation", "Train arriving at a station", "Elderly couple checking engine of automobile", and "Helicopter landing on the street".

C. Human Preference Annotation

C.1. Human Annotation Procedures

Labeling Instructions. To systematically communicate with human annotators about labeling rules, we prepare a labeling instruction document for each of the 16 dimensions. Each labeling instruction document consists of several important elements. First, we introduce the labeling user interface (shown in Figure 4 of the main paper), including the two videos in comparison, the location of prompts and questions, the control for video playback and stop, and the three choices to make (*i.e.*, "A is better", "B is better", or "Same quality"). Second, we explain the dimension of interest. Since we want to verify the human alignment of VBench in each fine-grained dimension, we conduct the labeling of different dimensions separately. In each document, we elaborate on the definition of the current dimension, including aspects to consider or discard. For instance, for the *Subject Consistency* dimension, annotators are asked to only focus on the look of the main subject, and not to consider the degree of temporal flickering, or the video alignment with the text prompt, and many other irrelevant dimensions. Each aspect to consider or discard is illustrated by both text descriptions and examples of synthesized videos. Third, we categorize various scenarios that annotators may encounter while annotating this dimension (*e.g.*, what is considered as "better", and what is considered as "same quality"). For each scenario, we provide explanatory examples.

Quality Assurance in Preference Annotations. To guarantee the accuracy of human preference annotations, we implement a systematic five-step approach: ***1)*** Labeling Instructions Preparation: For each evaluation dimension, we provide clear and well-organized labeling instructions with examples. ***2)*** Pre-Labeling Trial: Prior to the main annotation task, we conduct a pre-labeling trial, where annotators are assigned to annotate only 60 samples. We go through all 60 annotations and communicate with annotators about each wrong label, and clarify any misunderstanding or potential doubts in the labeling instructions. ***3)*** Labeling In-

structions Update: We update the labeling instructions according to feedback from the human annotators, and supplement the wrongly labeled samples into the labeling instructions. ***4)*** Post-Labeling Checks by Annotators: Upon labeling all samples for a particular dimension, the samples are grouped as 60 samples per package. In each package of 60 samples, human annotators go through 20% of randomly selected samples for quality checking. If for any package the error rate exceeds 10%, the entire package is sent back for re-labeling conducted by a different annotator. ***5)*** Post-Labeling Checks by Authors: Upon labeling and possible re-labelings, we conduct the same post-labeling checks procedure similar to step 4. For any labeling errors spotted, we communicate with the human annotator for correction, and ask them to go through the entire package again. If any package reports an error rate higher than 10%, the entire labeled samples (all packages) for this dimension are considered invalid. We communicate with human annotators regarding possible problems encountered during annotation, and go back to step 1 to conduct annotation for this dimension all over again.

C.2. VLM Tuning

VLM Tuning. Our human preference annotations are mainly used to validate the alignment of VBench evaluations with human perception in each dimension. We show that these annotations have the potential to be used for broader applications, such as fine-tuning VLM models to align more closely with human preferences. VideoChat [36] uses a pre-trained video encoder and a large language model to align and train video VLM with instruction data. We organize data from VBench for fine-tuning, enhancing the model's ability to assess video generation. By utilizing instruction data of the VBench Dataset coupled with human preference tags, VLM, through its cognitive chain, is with its Chain of Thought to choose suitable evaluation metrics and furnishing scores in accordance. Upon giving the prompt into the VLM and asking: "`Give the appropriate evaluation metrics`", we obtain the dimensions to be evaluated from Chain of Thought, as shown in Table A3. We feed the derived metrics along with the video into the VLM, and ask two additional questions: "`Please observe the video and describe it based on the provided metrics.`" and "`Predict the assessment score of the video within these metrics.`" We show examples of before and after VLM Tuning in Figure A18

Data Preparation. We organize human preference annotations and model scores across different dimensions into training datasets. For model scores, each video's ratings are mapped from 0-1 to a 0-10 scale and are coupled with questions used for human annotation to form our instruction data. Evaluations of different aspects of the same video are grouped to facilitate the VLM's ability to engage in multi-turn dialogues. As for human preference annotations, pairs of videos along with corresponding questions and preference options are organized into instruction data, thereby somewhat enhancing the model with the capability to make evaluative judgments.

Implementation Details Our approach uses VideoChat-embed [36] as the baseline model. The model undergoes fine-tuning on a set of 30,000 instruction pairs. We fine-tune the model for 3 epochs using a learning rate of 2e-5 and an overall batch size of 64. The training for our model takes about one hour when performed on 8 A100-80GB GPUs.

`<SYSTEM>:` You are an assistant with fair and objective standards for video assessment. Given the input statement for the video generation model: `{input text}`, please select appropriate evaluation dimensions from `['subject consistency', 'background consistency', 'temporal flickering', 'motion smoothness', 'dynamic degree', 'aesthetic quality', 'imaging quality', 'object class', 'multiple objects', 'human action', 'color', 'spatial relationship', 'scene', 'temporal style', 'appearance style', 'overall consistency'].`
`<USER>:` a dilapidated phone booth stood as a relic of a bygone era on the sidewalk, frozen in time. `<ASSISTANT>:` Based on the input statement, the following evaluation dimensions may be relevant: `subject consistency, background consistency, temporal flickering, motion smoothness, dynamic degree, aesthetic quality, imaging quality, scene, temporal style, overall consistency`

Table A3. **VLM Chain of Thought.** VLM suggests appropriate evaluation dimensions based on the user-input video prompt.

D. More Implementation Details

D.1. Video Generation Models in Evaluation

To evaluate our benchmark on recent advances, we adopt four models for comparison, and more will be added as they become open-sourced. Details of models and sampling

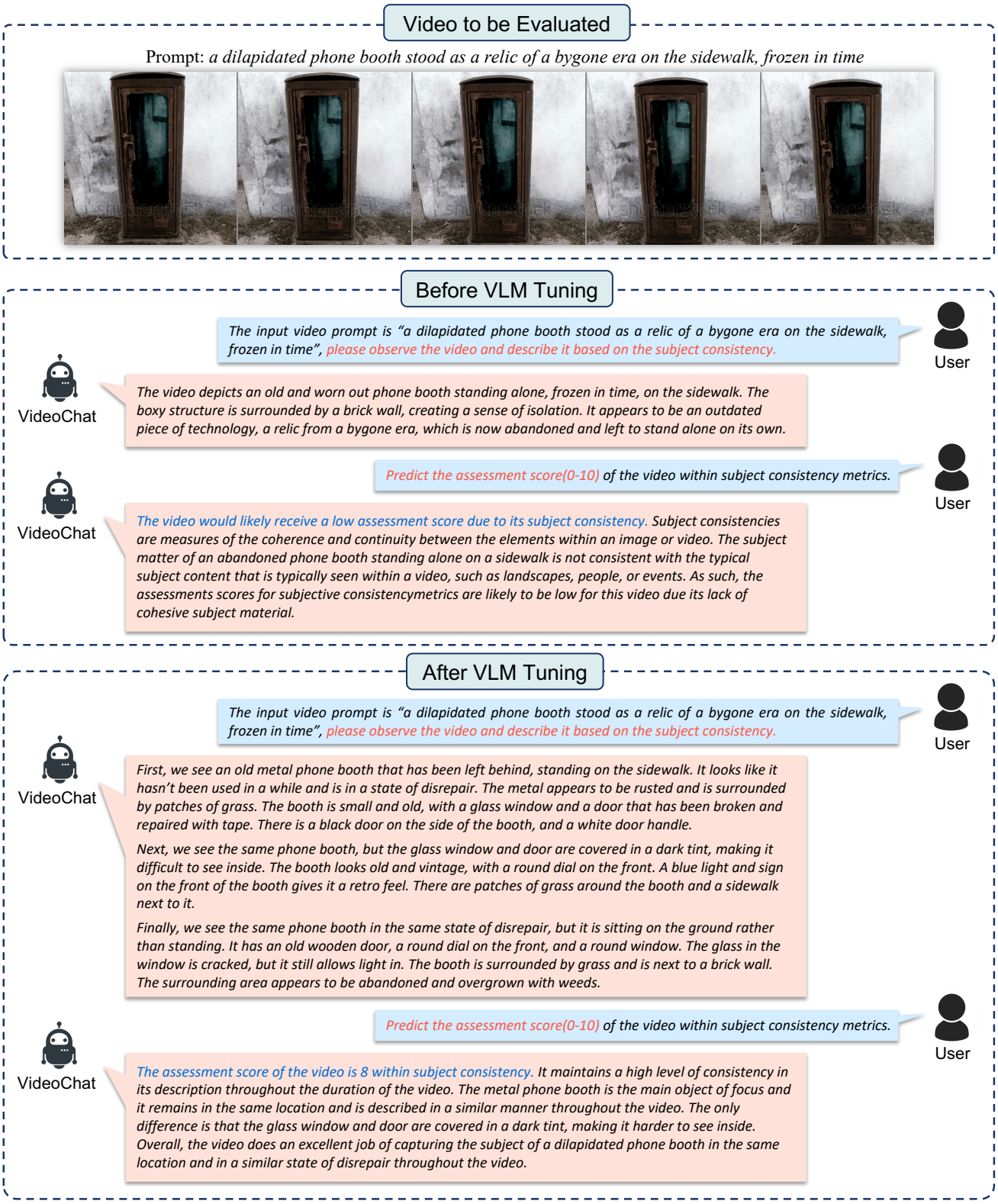

Figure A18. **VLM Tuning Example.** We use human preference annotation to fine-tune a VLM, and demonstrate that such fine-tuning can improve VLM's ability in evaluating video generation capabilities in specific dimensions.

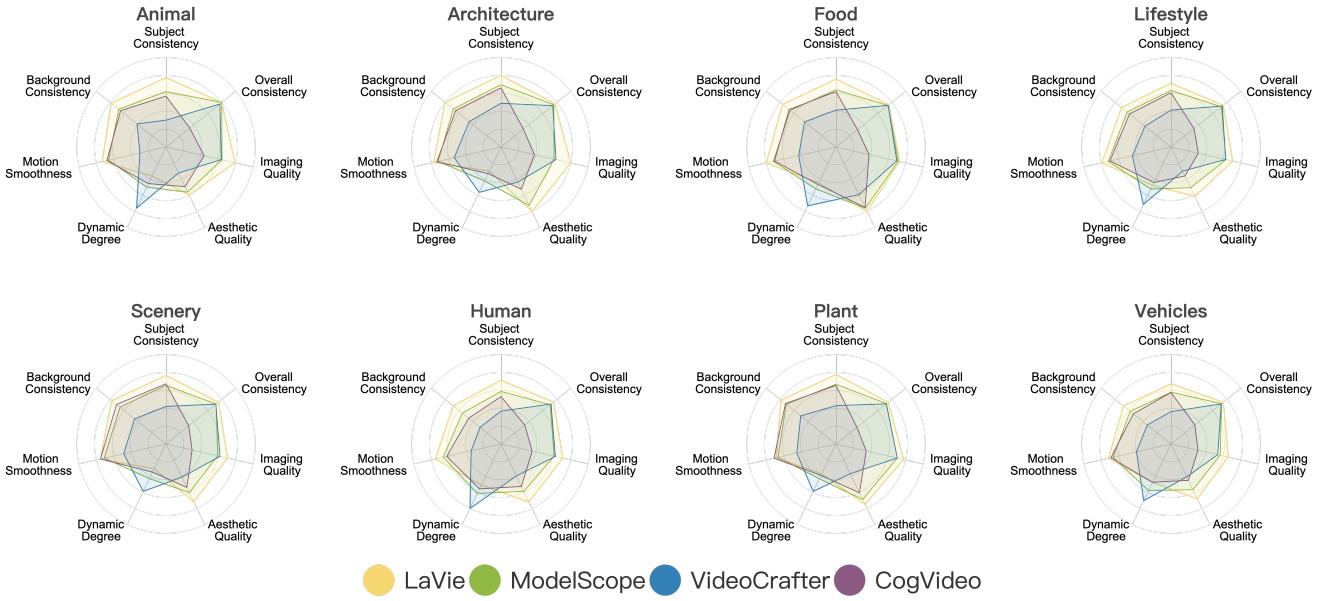

Figure A19. **VBench Results across Eight Content Categories (by Category per Chart)** (best viewed in color). For each chart, we plot the VBench evaluation results across different models on the same content category.

Table A4. **Validate VBench's Human Alignment.** We report *VBench Win Ratios (left) / Human Win Ratios (right)* for each dimension and each model. Our experiments show that VBench evaluations across all dimensions closely match human perceptions.

Models	Subject Consistency	Background Consistency	Temporal Flickering	Motion Smoothness	Dynamic Degree	Aesthetic Quality	Imaging Quality	Object Class
LaVie [61]	**67.87% / 69.95%**	**80.08% / 65.04%**	**73.42% / 87.96%**	**69.54% / 65.65%**	41.81% / 53.10%	**77.56% / 83.41%**	**77.20% / 79.46%**	**57.55% / 79.20%**
ModelScope [42, 56]	49.07% / 56.30%	46.82% / 56.36%	65.42% / 62.44%	58.61% / 59.58%	52.92% / 53.84%	67.74% / 63.15%	60.00% / 68.53%	49.37% / 49.58%
VideoCrafter [23]	24.72% / 20.42%	13.95% / 27.21%	31.20% / 43.64%	10.00% / 13.80%	**68.47% / 62.18%**	35.34% / 32.33%	55.05% / 37.85%	54.18% / 41.77%
CogVideo [25]	58.33% / 53.33%	59.15% / 51.40%	29.96% / 5.96%	61.85% / 60.97%	36.81% / 30.88%	19.35% / 21.11%	7.74% / 14.16%	38.90% / 29.45%
Correlation	96.51%	94.12%	88.73%	99.80%	82.09%	98.65%	92.16%	80.37%
Models	**Multiple Objects**	**Human Action**	**Color**	**Spatial Relationship**	**Scene**	**Appearance Style**	**Temporal Style**	**Overall Consistency**
LaVie [61]	53.37% / 57.97%	**54.43% / 58.13%**	**52.31% / 51.37%**	52.30% / 49.81%	**59.69% / 77.52%**	**61.85% / 58.22%**	**69.07%** / 55.73%	**70.82% / 77.35%**
ModelScope [42, 56]	**57.15% / 62.15%**	51.10% / 53.07%	50.12% / 49.73%	53.25% / 53.15%	48.22% / 50.00%	57.48% / 54.93%	65.40% / **57.50%**	66.31% / 60.07%
VideoCrafter [23]	48.74% / 49.63%	52.17% / 47.87%	48.71% / 47.92%	**56.11% / 54.66%**	52.79% / 46.05%	36.67% / 40.07%	65.40% / 51.90%	62.65% / 48.10%
CogVideo [25]	40.73% / 30.24%	42.30% / 40.93%	48.86% / 50.98%	38.33% / 42.38%	39.30% / 26.43%	44.00% / 46.78%	0.13% / 34.87%	0.22% / 14.48%
Correlation	98.98%	89.15%	60.73%	97.59%	94.07%	99.65%	97.53%	93.27%

Table A5. **VBench Evaluation Results on the WebVid-Avg Reference Baseline.** This table shows the VBench evaluation results on the *WebVid-Avg* baseline. We provide results from other models and baselines as well for a comprehensive view.

Models	Subject Consistency	Background Consistency	Motion Smoothness	Dynamic Degree	Aesthetic Quality	Imaging Quality	Appearance Style	Temporal Style	Overall Consistency
LaVie [61]	91.41%	**97.47%**	96.38%	49.72%	**54.94%**	**61.90%**	**23.56%**	**25.93%**	**26.41%**
ModelScope [42, 56]	89.87%	95.29%	95.79%	66.39%	52.06%	58.57%	23.39%	25.37%	25.67%
VideoCrafter [23]	86.24%	92.88%	91.79%	**89.72%**	44.41%	57.22%	21.57%	25.42%	25.21%
CogVideo [25]	**92.19%**	96.20%	**96.47%**	42.22%	38.18%	41.03%	22.01%	7.80%	7.70%
Empirical Min	14.62%	26.15%	70.60%	0.00%	0.00%	0.00%	0.09%	0.00%	0.00%
WebVid Avg	96.17%	96.59%	98.17%	44.13%	42.37%	58.22%	22.15%	25.77%	34.14%
Empirical Max	100.00%	100.00%	99.75%	100.00%	100.00%	100.00%	28.55%	36.40%	36.40%

Table A6. **VBench Results across Eight Content Categories.** We show the VBench evaluation results on the four T2V models, across eight content categories, on various evaluation dimensions.

Models	Categories	Subject Consistency	Background Consistency	Motion Smoothness	Dynamic Degree	Aesthetic Quality	Imaging Quality	Overall Consistency
LaVie [61]	**Animal**	97.49%	97.18%	97.29%	15.20%	48.26%	68.81%	**26.43%**
	Architecture	**98.04%**	**97.38%**	97.83%	5.20%	**54.20%**	**69.30%**	25.46%
	Food	97.11%	96.90%	**98.18%**	28.80%	54.15%	65.24%	24.88%
	Lifestyle	96.10%	96.19%	98.08%	33.60%	48.76%	64.02%	24.43%
	Scenery	97.27%	97.06%	97.58%	6.40%	51.76%	63.86%	24.56%
	Human	96.11%	95.88%	97.57%	**39.00%**	51.87%	64.07%	24.63%
	Plant	97.52%	97.20%	96.73%	16.40%	52.68%	67.86%	24.50%
	Vehicles	95.23%	95.82%	97.11%	34.00%	50.70%	61.02%	24.51%
ModelScope [42, 56]	**Animal**	94.08%	95.80%	96.40%	37.20%	47.32%	60.30%	**26.58%**
	Architecture	**95.77%**	95.88%	**97.20%**	24.80%	52.10%	58.38%	24.89%
	Food	94.53%	95.53%	97.17%	40.80%	**53.06%**	**64.39%**	24.40%
	Lifestyle	94.36%	95.17%	97.18%	41.00%	45.77%	59.62%	23.51%
	Scenery	94.88%	95.57%	97.03%	26.00%	48.57%	57.49%	23.28%
	Human	93.37%	94.21%	96.45%	**56.00%**	48.14%	58.41%	22.84%
	Plant	95.14%	**96.26%**	96.48%	26.40%	51.03%	63.83%	23.55%
	Vehicles	93.17%	94.61%	96.47%	50.20%	47.53%	55.75%	23.60%
VideoCrafter [23]	**Animal**	87.01%	92.40%	91.80%	79.60%	40.51%	59.79%	**25.47%**
	Architecture	**91.18%**	92.93%	**94.83%**	47.80%	43.71%	59.63%	24.27%
	Food	89.50%	92.87%	93.44%	75.00%	**48.19%**	63.47%	24.47%
	Lifestyle	89.51%	91.87%	93.63%	72.20%	39.84%	59.44%	24.01%
	Scenery	89.67%	92.86%	94.17%	51.80%	43.06%	58.98%	23.20%
	Human	88.50%	90.92%	92.35%	**86.20%**	42.62%	59.23%	23.31%
	Plant	89.86%	**93.57%**	93.72%	52.00%	41.81%	**63.81%**	23.41%
	Vehicles	88.38%	91.44%	93.04%	70.60%	42.95%	54.14%	23.39%
CogVideo [25]	**Animal**	92.95%	95.45%	96.65%	30.20%	45.37%	**48.45%**	8.26%
	Architecture	95.00%	95.45%	97.39%	10.20%	46.29%	45.33%	7.48%
	Food	94.08%	95.73%	96.99%	32.00%	**52.79%**	45.05%	7.01%
	Lifestyle	93.80%	94.71%	96.93%	28.00%	41.57%	41.28%	7.85%
	Scenery	**95.27%**	96.21%	**97.58%**	13.20%	46.72%	40.49%	7.66%
	Human	92.08%	93.03%	95.93%	**46.80%**	46.38%	43.81%	8.29%
	Plant	94.86%	**96.41%**	97.05%	19.60%	48.63%	43.22%	6.65%
	Vehicles	93.11%	94.02%	96.80%	33.60%	44.18%	41.05%	**8.34%**

strategy are listed as follows.

LaVie. LaVie [61] is a high-quality video generation model that incorporates cascaded latent diffusion models. Specifically, a set of temporal modules is attached to the vanilla Stable Diffusion [51] model and the entire model is jointly trained on both images and videos to achieve video generation. For each prompt, we sample 16 continuous frames of size 512×512 at 8 frames per second (FPS). We use the DDPM sampling of 250 steps. The initial random seed is set to 2 and the classifier-free guidance is set to 7.

ModelScope. ModelScope [42, 56] is a diffusion-based text-to-video generation model. We adopt its official inference code and sample 16 frames of size 256×256 at 8 FPS.

VideoCrafter. VideoCrafter [23] is a toolkit for text-to-video generation and editing. We adopt the VideoCrafter 0.9 version (*a.k.a.*, LVDM) and utilize its base generic text-to-video generation model. We use the official inference code to sample 16 frames of size 256×256 at 8 FPS. The initial random seed is set to 2 during sampling.

CogVideo. CogVideo [25] is a transformer-based text-to-video generation model that inherits the pretrained text-to-image model CogView2 [15]. Since the official inference code requires simplified Chinese input, we translate all prompts into Chinese. We sample 33 frames of size 480×480 at 10 FPS for each video, according to its default settings. During sampling, all stages are involved in the pipelines, including sequential generation, frame interpolation, and recursive interpolation. The initial random seed is also set to 2 for a fair comparison.

D.2. Reference Baselines

In the main paper, we devise the *Empirical Max* and *Empirical Min* baselines to approximate the maximum / minimum scores that videos might be able to achieve. We also devise the *WebVid-Avg* baseline to reflect the average video quality of WebVid-10M dataset [5] as a reference. The numerical

results are displayed in Table 1 in the main paper, and Table A5 in this Supplementary File. We provide additional details on approximating these values as follows.

Empirical Max. *(1) WebVid-10M's Maximum.* For dimensions where the 100% score is unlikely to be achieved by any video, we retrieve WebVid-10M's real videos and report the highest-scoring video's result. Examples of such dimensions include *Motion Smoothness*, *Scene*, *Appearance Style*, *Temporal Style*, and *Overall Consistency*. *(2) Theoretical 100%.* For dimensions where there exist videos that can achieve 100%, we directly use 100% as the empirical maximum value. For temporal consistency dimensions *Subject Consistency*, *Background Consistency*, and *Temporal Flickering*, a completely static video corresponds to the 100% score. For *Dynamic Degree*, a set of highly dynamic videos can achieve the 100% ratio of dynamic degree. For the frame-wise quality dimensions *Aesthetic Quality* and *Imaging Quality*, a video consisting of 100%-scoring frames results in a final 100% score. For video-text semantics dimensions *Object Class*, *Multiple Objects*, *Human Actions*, *Color*, and *Spatial Relationship*, videos with the correct semantics specified in the text prompt can score 100%.

Empirical Min. *(1) Gaussian Noise Videos.* For video-text feature similarity dimensions *Appearance Style*, *Temporal Style*, and *Overall Consistency*, we use videos of i.i.d. Gaussian noise and the corresponding prompt suites to compute the corresponding score, and select the smallest value as the approximated empirical minimum (with some actually reaching 0%). For *Temporal Flickering* and *Motion Smoothness*, we directly compute the score of the Gaussian noise videos and take the minimum scoring video's result. For *Human Action*, our method suite gives 0% on the Gaussian noise videos. *(2) Composed Videos.* For temporal consistency dimensions *Subject Consistency* and *Background Consistency*, we randomly sample frames from different WebVid-10M [5] videos to form a video with dynamically shifting content. This procedure is repeated 1000 times, and the minimum score among all videos obtained serves as the empirical minimum reference. *(3) Theoretical 0%.* For dimensions where there exist videos that can achieve 0%, we directly use 0% as the empirical minimum value. For *Dynamic Degree*, a set of static videos can achieve the 0% ratio of dynamic degree. For the frame-wise dimensions *Aesthetic Quality* and *Imaging Quality*, a video consisting of 0%-scoring frames results in a final 0% score. For video-text semantics dimensions *Object Class*, *Multiple Objects*, *Color*, *Spatial Relationship*, and *Scene*, videos with the incorrect semantics specified in the text prompt can score 100%.

WebVid-Avg. For dimensions where WebVid-10M videos can be retrieved with high confidence according to their captions, such as *Subject Consistency*, *Background Consistency*, *Motion Smoothness*, *Dynamic Degree*, *Aesthetic Quality*, *Imaging Quality*, *Appearance Style*, *Temporal Style*, and *Overall Consistency*, we compute the average score for all retrieved videos in relation to the corresponding dimension. This average score serves as a reference value for the average of real videos. The results are visualized in the main paper Figure 6 (b), and detailed in Table A5 in this Supplementary File.

D.3. Normalization for Radar Chart Visualization

In the radar charts, we perform normalization to clearly visualize the relative performance. We detail the normalization methods as follows:

- *Main Paper Figure 2. VBench Evaluation Results of Video Generative Models* - For each dimension, we map the maximum score achieved by one of the T2V models to 0.8, and the minimum score to 0.3, and linearly map the remaining models' scores to the radar chart axes. The radar chart axes have a range from 0.0 to 1.0.
- *Main Paper Figure 6 (a). T2V vs. T2I* - For each dimension, we map the maximum score achieved by one of the models (including T2I and T2V models) to 0.8, and the minimum score to 0.3, and linearly map the remaining models' scores to the radar chart axes. The radar chart axes have a range from 0.0 to 1.0.
- *Main Paper Figure 6 (b). T2V vs. WebV-Avg & Max* - For each dimension, we map the maximum score achieved by one of the models (including the *Empirical Max* and *WebVid-Avg* baselines) to 0.8, and the minimum score to 0.3, and linearly map the remaining models' scores to the radar chart axes. The radar chart axes have a range from 0.0 to 1.0.
- *Main Paper Figure 7. VBench Results across Eight Content Categories (by Model)* - For each dimension, there are 32 numerical results corresponding to the four T2V models and eight content categories. We map the maximum score among the 32 results to 1.0, and the minimum score among the 32 results to 0.0, and linearly map the remaining 30 scores to respective radar charts' axes. The radar chart axes have a range from 0.0 to 1.0.
- *Supp File Figure A19. VBench Results across Eight Content Categories (by Category)* - Unlike Figure 7 in the main paper which put different categories of the same model in one radar chart, in Figure A19 we use an alternative visualization method, that is, collecting different models' results of the same category in one radar chart. For each dimension, there are 32 numerical results corresponding to the four T2V models and eight content categories. We map the maximum score among the 32 results to 0.8, and the minimum score among the 32 results to 0.3, and linearly map the remaining 30 scores to respective radar charts' axes. The radar chart axes have a range from 0.0 to 1.0.

Table A7. **VBench Evaluation Results of Video vs. Image Generation Models.** We compare the performance of four video generation models against three image generation models. For each evaluation dimension, a higher score represents relatively better performance. For *Overall Consistency* we replaced the ViCLIP approach by CLIP to enable evaluating image generation models.

Models	Aesthetic Quality	Imaging Quality	Object Class	Multiple Objects	Human Action	Color	Spatial Relationship	Scene	Appearance Style	Overall Consistency
LaVie [61]	54.94%	61.90%	91.82%	33.32%	**96.80%**	86.39%	34.09%	52.69%	23.56%	32.96%
ModelScope [42, 56]	52.06%	58.57%	82.25%	38.98%	92.40%	81.72%	33.68%	39.26%	23.39%	31.99%
VideoCrafter [23]	44.41%	57.22%	87.34%	25.93%	93.00%	78.84%	36.74%	43.36%	21.57%	30.78%
CogVideo [25]	38.18%	41.03%	73.40%	18.11%	78.20%	79.57%	18.24%	28.24%	22.01%	27.80%
SD1.4 [51]	65.85%	**69.86%**	91.14%	34.39%	91.80%	90.57%	61.89%	52.33%	25.35%	32.59%
SD2.1 [51]	66.50%	69.10%	**93.42%**	51.22%	89.00%	**91.15%**	73.11%	**58.14%**	**25.48%**	33.08%
SDXL [48]	**70.38%**	68.79%	91.39%	**69.51%**	91.20%	88.92%	**86.17%**	54.65%	25.23%	**33.77%**

E. Potential Negative Societal Impacts

Video generation models could be maliciously applied to generate fake content involving human figures. Moreover, generative models can potentially inherit biases from the training datasets [16]. Therefore, we recognize the importance of considering ethical and safety aspects when evaluating video generation models. We plan to include safety and equality dimensions in future iterations of VBench. We also urge users to apply video generation models with discretion.

F. Limitations and Future Work

Limited Amount of Open-Sourced T2V Models: Currently, the number of open-sourced T2V models are still limited. We will open-source our VBench and encourage more T2V models to participate in the evaluation, including but not limited to [1–4, 6, 72], so that we can provide more informed insights into the current state of T2V, and provide more annotated data on T2V generation results generated by different models.

Evaluation of Other Video Generation Tasks: Text-to-video (T2V) is a fundamental task in video generation, and there are other related video generation tasks such as video-driven (*i.e.*, video editing) [8, 9, 14, 20, 27, 33, 35, 39, 41, 45, 47, 49, 58, 66, 68, 69, 75–77], image-driven (*i.e.*, image-to-video) [10, 12, 17, 19, 21, 45, 46, 53, 54, 57, 59, 63, 64, 70, 71], personalized video generation [22, 24, 30, 77], and other types of multi-modal-controlled video synthesis [11, 13, 26, 30, 33, 43, 44, 57, 60, 66, 67, 73, 74]. We build our VBench towards T2V as the initial step, and plan to extend our benchmark suite to accommodate other modalities' controls by adding towards the "*Video-Condition Consistency*" dimensions. Our "*Video Quality*" dimensions are readily available for evaluating these video generation tasks.

G. Additional Experimental Results

In this section, we provide additional numerical results that correspond to the main paper visualizations. We list the resulting tables and figures as follows:

- In Table A7, we show the VBench evaluation results of four video generation models and three image generation models, further illustrating through numerical results the significant differences that exist in certain dimensions between video generation models and image generation models (corresponding to *main paper Figure 6 (a)*). For *Overall Consistency* we replaced the ViCLIP approach by CLIP to enable evaluating image generation models.
- In Table A4, we show the win ratio on evaluation results predicted by VBench and Human across four models and all dimensions, along with the correlation (ρ) between Human and VBench results (corresponding to *main paper Figure 5*).
- In Table A5, we show the results of WebVid-Avg and compare them with the results of four models and other reference baselines (corresponding to *main paper Figure 6 (b)*).
- In Table A6, we show all the evaluation results of VBench across four models and eight different categories, providing numerical support for the relevant observations in the insights. (corresponding to *main paper Figure 7*). Additionally, for the *Dynamic Degree* dimension, intrinsic attributes of different categories naturally result in noticeable differences in the dynamic degrees among various categories. For instance, the `Human` category consistently exhibits the highest *dynamic degree* across different models. Conversely, the `Architecture`, `Scenery`, and `Plant` categories consistently showcase the lowest *dynamic degree* across various models, and the ascending order from lowest to highest remains consistent as `Architecture`, `Scenery`, and `Plant`. Due to this characteristic, the dynamic degree shows significant variability across different categories. Therefore, we isolate it as a supplementary dimension for additional analysis on top of other

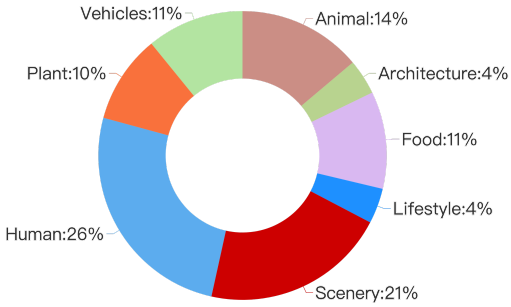

Figure A20. **WebVid-10M Dataset Categorical Distribution.** We visualize the percentage of data amount of each of the eight content categories in the WebVid-10M dataset.

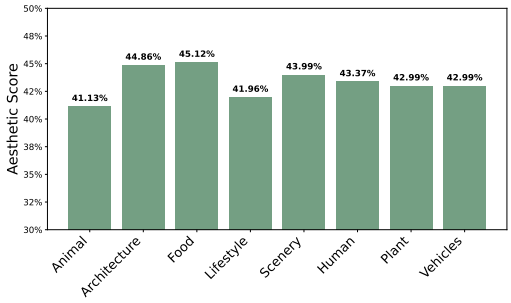

Figure A21. **Aesthetic Quality for Eight Categories in WebVid-10M dataset.** We visualize the aesthetic score of each of the eight content categories in the WebVid-10M dataset.

dimensions.

- In Figure A20, we show the statistical distribution of data amount of each of the eight content categories in the WebVid-10M dataset (supporting observations and insights mentioned in the *main paper Section 5*).
- In Figure A21, we show the aesthetic scores of eight different categories within the WebVid-10M dataset (supporting observations and insights mentioned in the *main paper Section 5*).

References

[1] Gen-2. Accessed September 25, 2023 [Online] https://research.runwayml.com/gen2, 2023. 14

[2] Morph studio. Accessed September 25, 2023 [Online] https://www.morphstudio.com/, 2023.

[3] Pika labs. Accessed September 25, 2023 [Online] https://www.pika.art/, 2023.

[4] Zeroscope-xl. Accessed September 25, 2023 [Online] https://huggingface.co/cerspense/zeroscope_v2_XL, 2023. 14

[5] Max Bain, Arsha Nagrani, Gül Varol, and Andrew Zisserman. Frozen in time: A joint video and image encoder for end-to-end retrieval. In *ICCV*, 2021. 12, 13

[6] Andreas Blattmann, Robin Rombach, Huan Ling, Tim Dockhorn, Seung Wook Kim, Sanja Fidler, and Karsten Kreis. Align your latents: High-resolution video synthesis with latent diffusion models. In *CVPR*, 2023. 14

[7] Mathilde Caron, Hugo Touvron, Ishan Misra, Hervé Jégou, Julien Mairal, Piotr Bojanowski, and Armand Joulin. Emerging properties in self-supervised vision transformers. In *ICCV*, 2021. 1

[8] Duygu Ceylan, Chun-Hao P Huang, and Niloy J Mitra. Pix2video: Video editing using image diffusion. In *ICCV*, 2023. 14

[9] Wenhao Chai, Xun Guo, Gaoang Wang, and Yan Lu. Stablevideo: Text-driven consistency-aware diffusion video editing. *arXiv preprint arXiv:2308.09592*, 2023. 14

[10] Tsai-Shien Chen, Chieh Hubert Lin, Hung-Yu Tseng, Tsung-Yi Lin, and Ming-Hsuan Yang. Motion-conditioned diffusion model for controllable video synthesis. *arXiv preprint arXiv:2304.14404*, 2023. 14

[11] Weifeng Chen, Jie Wu, Pan Xie, Hefeng Wu, Jiashi Li, Xin Xia, Xuefeng Xiao, and Liang Lin. Control-a-video: Controllable text-to-video generation with diffusion models. *arXiv preprint arXiv:2305.13840*, 2023. 14

[12] Xinyuan Chen, Yaohui Wang, Lingjun Zhang, Shaobin Zhuang, Xin Ma, Jiashuo Yu, Yali Wang, Dahua Lin, Yu Qiao, and Ziwei Liu. Seine: Short-to-long video diffusion model for generative transition and prediction. *arXiv preprint arXiv:2310.20700*, 2023. 14

[13] Ernie Chu, Shuo-Yen Lin, and Jun-Cheng Chen. Video controlnet: Towards temporally consistent synthetic-to-real video translation using conditional image diffusion models. *arXiv preprint arXiv:2305.19193*, 2023. 14

[14] Paul Couairon, Clément Rambour, Jean-Emmanuel Haugeard, and Nicolas Thome. Videdit: Zero-shot and spatially aware text-driven video editing. *arXiv preprint arXiv:2306.08707*, 2023. 14

[15] Ming Ding, Wendi Zheng, Wenyi Hong, and Jie Tang. Cogview2: Faster and better text-to-image generation via hierarchical transformers. In *NeurIPS*, 2022. 12

[16] Patrick Esser, Robin Rombach, and Björn Ommer. A note on data biases in generative models. In *NeurIPS Workshop*, 2020. 14

[17] Patrick Esser, Johnathan Chiu, Parmida Atighehchian, Jonathan Granskog, and Anastasis Germanidis. Structure and content-guided video synthesis with diffusion models. In *ICCV*, 2023. 14

[18] Yuming Fang, Hanwei Zhu, Yan Zeng, Kede Ma, and Zhou Wang. Perceptual quality assessment of smartphone photography. In *CVPR*, 2020. 4

[19] Tsu-Jui Fu, Licheng Yu, Ning Zhang, Cheng-Yang Fu, Jong-Chyi Su, William Yang Wang, and Sean Bell. Tell me what happened: Unifying text-guided video completion via multimodal masked video generation. In *CVPR*, 2023. 14

[20] Michal Geyer, Omer Bar-Tal, Shai Bagon, and Tali Dekel. Tokenflow: Consistent diffusion features for consistent video editing. *arXiv preprint arxiv:2307.10373*, 2023. 14

[21] Xianfan Gu, Chuan Wen, Jiaming Song, and Yang Gao. Seer: Language instructed video prediction with latent diffusion models. *arXiv preprint arXiv:2303.14897*, 2023. 14

[22] Yuwei Guo, Ceyuan Yang, Anyi Rao, Yaohui Wang, Yu Qiao, Dahua Lin, and Bo Dai. Animatediff: Animate your personalized text-to-image diffusion models without specific tuning. In *ICLR*, 2024. 14

[23] Yingqing He, Tianyu Yang, Yong Zhang, Ying Shan, and Qifeng Chen. Latent video diffusion models for high-fidelity video generation with arbitrary lengths. *arXiv preprint arXiv:2211.13221*, 2022. 2, 11, 12, 14

[24] Yingqing He, Menghan Xia, Haoxin Chen, Xiaodong Cun, Yuan Gong, Jinbo Xing, Yong Zhang, Xintao Wang, Chao Weng, Ying Shan, et al. Animate-a-story: Storytelling with retrieval-augmented video generation. *arXiv preprint arXiv:2307.06940*, 2023. 14

[25] Wenyi Hong, Ming Ding, Wendi Zheng, Xinghan Liu, and Jie Tang. CogVideo: Large-scale pretraining for text-to-video generation via transformers. *arXiv preprint arXiv:2205.15868*, 2022. 2, 11, 12, 14

[26] Zhihao Hu and Dong Xu. Videocontrolnet: A motion-guided video-to-video translation framework by using diffusion model with controlnet. *arXiv preprint arXiv:2307.14073*, 2023. 14

[27] Jiahui Huang, Leonid Sigal, Kwang Moo Yi, Oliver Wang, and Joon-Young Lee. Inve: Interactive neural video editing. *arXiv preprint arXiv:2307.07663*, 2023. 14

[28] Kaiyi Huang, Kaiyue Sun, Enze Xie, Zhenguo Li, and Xihui Liu. T2i-compbench: A comprehensive benchmark for open-world compositional text-to-image generation. *arXiv preprint arXiv: 2307.06350*, 2023. 5

[29] Xinyu Huang, Youcai Zhang, Jinyu Ma, Weiwei Tian, Rui Feng, Yuejie Zhang, Yaqian Li, Yandong Guo, and Lei Zhang. Tag2text: Guiding vision-language model via image tagging. *arXiv preprint arXiv:2303.05657*, 2023. 5

[30] Johanna Karras, Aleksander Holynski, Ting-Chun Wang, and Ira Kemelmacher-Shlizerman. Dreampose: Fashion image-to-video synthesis via stable diffusion. *arXiv preprint arXiv:2304.06025*, 2023. 14

[31] Will Kay, Joao Carreira, Karen Simonyan, Brian Zhang, Chloe Hillier, Sudheendra Vijayanarasimhan, Fabio Viola, Tim Green, Trevor Back, Paul Natsev, et al. The kinetics human action video dataset. *arXiv preprint arXiv:1705.06950*, 2017. 5, 7

[32] Junjie Ke, Qifei Wang, Yilin Wang, Peyman Milanfar, and Feng Yang. MUSIQ: multi-scale image quality transformer. *CoRR*, abs/2108.05997, 2021. 3

[33] Levon Khachatryan, Andranik Movsisyan, Vahram Tadevosyan, Roberto Henschel, Zhangyang Wang, Shant Navasardyan, and Humphrey Shi. Text2video-zero: Text-to-image diffusion models are zero-shot video generators. *arXiv preprint arXiv:2303.13439*, 2023. 14

[34] LAION-AI. aesthetic-predictor. https://github.com/LAION-AI/aesthetic-predictor, 2022. 3

[35] Yao-Chih Lee, Ji-Ze Genevieve Jang Jang, Yi-Ting Chen, Elizabeth Qiu, and Jia-Bin Huang. Shape-aware text-driven layered video editing demo. *arXiv preprint arXiv:2301.13173*, 2023. 14

[36] Kunchang Li, Yinan He, Yi Wang, Yizhuo Li, Wenhai Wang, Ping Luo, Yali Wang, Limin Wang, and Yu Qiao. Videochat: Chat-centric video understanding. *arXiv preprint arXiv:2305.06355*, 2023. 9

[37] Kunchang Li, Yali Wang, Yizhuo Li, Yi Wang, Yinan He, Limin Wang, and Yu Qiao. Unmasked teacher: Towards training-efficient video foundation models. *arXiv preprint arXiv:2303.16058*, 2023. 5

[38] Zhen Li, Zuo-Liang Zhu, Ling-Hao Han, Qibin Hou, Chun-Le Guo, and Ming-Ming Cheng. Amt: All-pairs multi-field transforms for efficient frame interpolation. In *CVPR*, 2023. 3

[39] Jun Hao Liew, Hanshu Yan, Jianfeng Zhang, Zhongcong Xu, and Jiashi Feng. Magicedit: High-fidelity and temporally coherent video editing. *arXiv preprint arXiv:2308.14749*, 2023. 14

[40] Tsung-Yi Lin, Michael Maire, Serge Belongie, James Hays, Pietro Perona, Deva Ramanan, Piotr Dollár, and C Lawrence Zitnick. Microsoft coco: Common objects in context. In *ECCV*, 2014. 6, 7

[41] Shaoteng Liu, Yuechen Zhang, Wenbo Li, Zhe Lin, and Jiaya Jia. Video-p2p: Video editing with cross-attention control. *arXiv preprint arXiv:2303.04761*, 2023. 14

[42] Zhengxiong Luo, Dayou Chen, Yingya Zhang, Yan Huang, Liang Wang, Yujun Shen, Deli Zhao, Jingren Zhou, and Tieniu Tan. VideoFusion: Decomposed diffusion models for high-quality video generation. In *CVPR*, 2023. 2, 11, 12, 14

[43] Yue Ma, Yingqing He, Xiaodong Cun, Xintao Wang, Ying Shan, Xiu Li, and Qifeng Chen. Follow your pose: Pose-guided text-to-video generation using pose-free videos. *arXiv preprint arXiv:2304.01186*, 2023. 14

[44] Guillaume Le Moing, Jean Ponce, and Cordelia Schmid. WALDO: Future video synthesis using object layer decomposition and parametric flow prediction. In *ICCV*, 2023. 14

[45] Eyal Molad, Eliahu Horwitz, Dani Valevski, Alex Rav Acha, Yossi Matias, Yael Pritch, Yaniv Leviathan, and Yedid Hoshen. Dreamix: Video diffusion models are general video editors. *arXiv preprint arXiv:2302.01329*, 2023. 14

[46] Haomiao Ni, Changhao Shi, Kai Li, Sharon X Huang, and Martin Renqiang Min. Conditional image-to-video generation with latent flow diffusion models. In *CVPR*, 2023. 14

[47] Hao Ouyang, Qiuyu Wang, Yuxi Xiao, Qingyan Bai, Juntao Zhang, Kecheng Zheng, Xiaowei Zhou, Qifeng Chen, and Yujun Shen. Codef: Content deformation fields for temporally consistent video processing. In *CVPR*, 2024. 14

[48] Dustin Podell, Zion English, Kyle Lacey, Andreas Blattmann, Tim Dockhorn, Jonas Müller, Joe Penna, and Robin Rombach. Sdxl: Improving latent diffusion models for high-resolution image synthesis. *arXiv preprint arXiv:2307.01952*, 2023. 3, 14

[49] Chenyang Qi, Xiaodong Cun, Yong Zhang, Chenyang Lei, Xintao Wang, Ying Shan, and Qifeng Chen. Fatezero: Fusing attentions for zero-shot text-based video editing. *arXiv preprint arXiv:2303.09535*, 2023. 14

[50] Alec Radford, Jong Wook Kim, Chris Hallacy, Aditya Ramesh, Gabriel Goh, Sandhini Agarwal, Girish Sastry, Amanda Askell, Pamela Mishkin, Jack Clark, et al. Learning transferable visual models from natural language supervision. In *ICML*, 2021. 1, 6

[51] Robin Rombach, Andreas Blattmann, Dominik Lorenz, Patrick Esser, and Björn Ommer. High-resolution image synthesis with latent diffusion models. In *CVPR*, 2022. 12, 14

[52] Nataniel Ruiz, Yuanzhen Li, Varun Jampani, Yael Pritch, Michael Rubinstein, and Kfir Aberman. Dreambooth: Fine tuning text-to-image diffusion models for subject-driven generation. In *CVPR*, 2023. 1

[53] Uriel Singer, Adam Polyak, Thomas Hayes, Xi Yin, Jie An, Songyang Zhang, Qiyuan Hu, Harry Yang, Oron Ashual, Oran Gafni, et al. Make-a-video: Text-to-video generation without text-video data. *arXiv preprint arXiv:2209.14792*, 2022. 14

[54] Xue Song, Jingjing Chen, Bin Zhu, and Yu-Gang Jiang. Text-driven video prediction. *arXiv preprint arXiv:2210.02872*, 2022. 14

[55] Zachary Teed and Jia Deng. Raft: Recurrent all-pairs field transforms for optical flow. In *ECCV*, 2020. 2, 3

[56] Jiuniu Wang, Hangjie Yuan, Dayou Chen, Yingya Zhang, Xiang Wang, and Shiwei Zhang. Modelscope text-to-video technical report. *arXiv preprint arXiv:2308.06571*, 2023. 2, 11, 12, 14

[57] Tan Wang, Linjie Li, Kevin Lin, Chung-Ching Lin, Zhengyuan Yang, Hanwang Zhang, Zicheng Liu, and Lijuan Wang. Disco: Disentangled control for referring human dance generation in real world. *arXiv preprint arXiv:2307.00040*, 2023. 14

[58] Wen Wang, kangyang Xie, Zide Liu, Hao Chen, Yue Cao, Xinlong Wang, and Chunhua Shen. Zero-shot video editing using off-the-shelf image diffusion models. *arXiv preprint arXiv:2303.17599*, 2023. 14

[59] Xiaodong Wang, Chenfei Wu, Shengming Yin, Minheng Ni, Jianfeng Wang, Linjie Li, Zhengyuan Yang, Fan Yang, Lijuan Wang, Zicheng Liu, et al. Learning 3d photography videos via self-supervised diffusion on single images. *arXiv preprint arXiv:2302.10781*, 2023. 14

[60] Xiang Wang, Hangjie Yuan, Shiwei Zhang, Dayou Chen, Jiuniu Wang, Yingya Zhang, Yujun Shen, Deli Zhao, and Jingren Zhou. Videocomposer: Compositional video synthesis with motion controllability. *arXiv preprint arXiv:2306.02018*, 2023. 14

[61] Yaohui Wang, Xinyuan Chen, Xin Ma, Shangchen Zhou, Ziqi Huang, Yi Wang, Ceyuan Yang, Yinan He, Jiashuo

Yu, Peiqing Yang, et al. Lavie: High-quality video generation with cascaded latent diffusion models. *arXiv preprint arXiv:2309.15103*, 2023. 2, 11, 12, 14

[62] Yi Wang, Yinan He, Yizhuo Li, Kunchang Li, Jiashuo Yu, Xin Ma, Xinyuan Chen, Yaohui Wang, Ping Luo, Ziwei Liu, Yali Wang, Limin Wang, and Yu Qiao. Internvid: A large-scale video-text dataset for multimodal understanding and generation. *arXiv preprint arXiv:2307.06942*, 2023. 6

[63] Yaohui Wang, Xin Ma, Xinyuan Chen, Antitza Dantcheva, Bo Dai, and Yu Qiao. Leo: Generative latent image animator for human video synthesis. *arXiv preprint arXiv:2305.03989*, 2023. 14

[64] Chenfei Wu, Jian Liang, Lei Ji, Fan Yang, Yuejian Fang, Daxin Jiang, and Nan Duan. Nüwa: Visual synthesis pre-training for neural visual world creation. In *ECCV*, 2022. 14

[65] Jialian Wu, Jianfeng Wang, Zhengyuan Yang, Zhe Gan, Zicheng Liu, Junsong Yuan, and Lijuan Wang. Grit: A generative region-to-text transformer for object understanding. *arXiv preprint arXiv:2212.00280*, 2022. 4

[66] Jay Zhangjie Wu, Yixiao Ge, Xintao Wang, Stan Weixian Lei, Yuchao Gu, Wynne Hsu, Ying Shan, Xiaohu Qie, and Mike Zheng Shou. Tune-a-video: One-shot tuning of image diffusion models for text-to-video generation. *arXiv preprint arXiv:2212.11565*, 2022. 14

[67] Jinbo Xing, Menghan Xia, Yuxin Liu, Yuechen Zhang, Yong Zhang, Yingqing He, Hanyuan Liu, Haoxin Chen, Xiaodong Cun, Xintao Wang, Ying Shan, and Tien-Tsin Wong. Make-your-video: Customized video generation using textual and structural guidance. *arXiv preprint arXiv:2306.00943*, 2023. 14

[68] Zhen Xing, Qi Dai, Han Hu, Zuxuan Wu, and Yu-Gang Jiang. Simda: Simple diffusion adapter for efficient video generation. *arXiv preprint arXiv:2308.09710*, 2023. 14

[69] Shuai Yang, Yifan Zhou, Ziwei Liu, and Chen Change Loy. Rerender a video: Zero-shot text-guided video-to-video translation. *arXiv preprint arXiv:2306.07954*, 2023. 14

[70] Shengming Yin, Chenfei Wu, Jian Liang, Jie Shi, Houqiang Li, Gong Ming, and Nan Duan. Dragnuwa: Fine-grained control in video generation by integrating text, image, and trajectory. *arXiv preprint arXiv:2308.08089*, 2023. 14

[71] Lijun Yu, Yong Cheng, Kihyuk Sohn, José Lezama, Han Zhang, Huiwen Chang, Alexander G Hauptmann, Ming-Hsuan Yang, Yuan Hao, Irfan Essa, et al. Magvit: Masked generative video transformer. In *CVPR*, 2023. 14

[72] David Junhao Zhang, Jay Zhangjie Wu, Jia-Wei Liu, Rui Zhao, Lingmin Ran, Yuchao Gu, Difei Gao, and Mike Zheng Shou. Show-1: Marrying pixel and latent diffusion models for text-to-video generation. *arXiv preprint arXiv:2309.15818*, 2023. 14

[73] Jianfeng Zhang, Hanshu Yan, Zhongcong Xu, Jiashi Feng, and Jun Hao Liew. Magicavatar: Multimodal avatar generation and animation. *arXiv preprint arXiv:2308.14748*, 2023. 14

[74] Yabo Zhang, Yuxiang Wei, Dongsheng Jiang, Xiaopeng Zhang, Wangmeng Zuo, and Qi Tian. Controlvideo: Training-free controllable text-to-video generation. *arXiv preprint arXiv:2305.13077*, 2023. 14

[75] Zicheng Zhang, Bonan Li, Xuecheng Nie, Congying Han, Tiande Guo, and Luoqi Liu. Towards consistent video editing with text-to-image diffusion models. *arXiv preprint arXiv:2305.17431*, 2023. 14

[76] Min Zhao, Rongzhen Wang, Fan Bao, Chongxuan Li, and Jun Zhu. Controlvideo: Adding conditional control for one shot text-to-video editing. *arXiv preprint arXiv:2305.17098*, 2023.

[77] Yuyang Zhao, Enze Xie, Lanqing Hong, Zhenguo Li, and Gim Hee Lee. Make-a-protagonist: Generic video editing with an ensemble of experts. *arXiv preprint arXiv:2305.08850*, 2023. 14

[78] Lianmin Zheng, Wei-Lin Chiang, Ying Sheng, Siyuan Zhuang, Zhanghao Wu, Yonghao Zhuang, Zi Lin, Zhuohan Li, Dacheng Li, Eric Xing, et al. Judging llm-as-a-judge with mt-bench and chatbot arena. *arXiv preprint arXiv:2306.05685*, 2023. 7

[79] Bolei Zhou, Agata Lapedriza, Jianxiong Xiao, Antonio Torralba, and Aude Oliva. Learning deep features for scene recognition using places database. In *NeurIPS*, 2014. 6